Fidelity-Commensurability Tradeoff in Joint Embedding of Disparate Dissimilarities

Sancar Adali[*]   Carey E. Priebe[†]

October 31, 2018

Abstract

In various data settings, it is necessary to compare observations from disparate data sources. We assume the data is in the dissimilarity representation [14] and investigate a joint embedding method [15] that results in a commensurate representation of disparate dissimilarities. We further assume that there are "matched" observations from different conditions which can be considered to be highly similar, for the sake of inference. The joint embedding results in the joint optimization of fidelity (preservation of within-condition dissimilarities) and commensurability (preservation of between-condition dissimilarities between matched observations). We show that the tradeoff between these two criteria can be made explicit using weighted raw stress as the objective function for multidimensional scaling. In our investigations, we use a weight parameter, w, to control the tradeoff, and choose match detection as the inference task. Our results show weights that are optimal (with respect to the inference task) are different than equal weights for commensurability and fidelity and the proposed weighted embedding scheme provides significant improvements in statistical power.

1   Introduction

We are interested in problems where the data sources are disparate and the inference task requires that observations from the different data sources be judged to be similar or dissimilar. By "disparate", we mean that the observations from the two sources are inherently incomparable, either because the data are of different modalities (such as images and text), or there is significant and unknown variability between the data sources (such as psychometric data collected from different

subjects). Throughout this paper, we refer to the disparateness of the observations when we mention they are from different "conditions".

Consider a collection of English Wikipedia articles and the hyperlink graph based on the links between the same articles. Each article corresponds to a vertex in this directed graph[1]. This correspondence illustrates our idea of "matchedness". This example also illustrates the idea of "disparate": there is no intuitive way to compare a text document and a vertex in a graph. We assume the training data consists of a collection of matched data from the disparate data sources.

The inference task we consider is match detection, i.e. deciding whether a new English article and a new vertex in the graph are matched. While a document can be compared with other documents in the same language via a dissimilarity measure defined for documents, and vertices in the same graph can be compared via a dissimilarity measure defined for graph vertices, a direct comparison between a document and a graph vertex is not possible. To facilitate our approach to the inference task at hand, it is necessary to derive a data representation where the observations from different conditions can be compared, i.e. the representation is commensurate. We will use a finite-dimensional Euclidean space for this commensurate representation, where standard statistical inference tools can be used.

As in the wikipedia document/graph example, it is possible that a feature representation of the data is not available or inference with such a representation is fraught with complications. This motivates our dissimilarity-centric approach. For an excellent resource on the usage of dissimilarities in pattern recognition, we refer the reader to the Pękalska and Duin book [14].

Since we proceed to inference starting from a dissimilarity representation of the data, our methodology may be applicable to any scenario in which multiple dissimilarity measures are available. Some illustrative examples include: pairs of images and their descriptive captions, photographs taken under different illumination conditions. In each case, we have an intuitive notion of matchedness: for photographs taken under different illumination conditions, "matched" means they are of the same person. For a collection of linked Wikipedia articles, the different conditions are the textual content and hyperlink graph structure, "matched" means a text document and a vertex in the graph corresponds to the same Wikipedia article.

To quantify how suitable the commensurate representation is for subsequent inference, two error criteria can be defined: *fidelity*, which refers to how well the available dissimilarities in a condition are preserved, and *commensurability*, which refers to how well the dissimilarities between matched objects are preserved. These two concepts will be made more concrete in section 4.

The major question addressed in this paper is whether, in the tradeoff between fidelity and commensurability, there is a "sweet spot": increases in fidelity (or commensurability) do not result in superior performance for the inference task, due to the resulting commensurability (or fidelity) loss.

2   Related Work

Our problem is very similar to the 3-way multidimensional scaling problem where the dissimilarity data is a $(n \times n \times K)$ tensor which represent pairwise dissimilarities between n objects as measured in K different conditions. However, whereas our

---

[1]For simplicity, assume the collection of articles correspond to a connected graph.

embedding approach finds a separate configuration of points for each condition, 3-way MDS methods [5, 7] find a *single* configuration of n points representing each object (which is referred to as "group space"), that is as consistent as possible with the dissimilarity data under different conditions. DISTATIS [1] accomplishes this goal by finding a compromise inner product matrix that is a weighted combination of the inner product matrices in different conditions. 3-way MDS methods such as INDSCAL [5], PROXSCAL [7] assume a common configuration in group space, from which the individual dissimilarity matrices are computed after being distorted by weight matrices. In contrast, when we adopt the joint "commensurate" embedding approach, the representation of the objects in the common space is never estimated. In fact, some of our inference tasks including match detection make sense only if we represent each object under each condition as a distinct point. The violation of global assumptions the INDSCAL and PROXSCAL methods make about the group space and the weight matrices might result in significant performance loss. Our method puts weaker constraints on the mapping between different conditions and allows the degree of matchedness to vary for different pairs of observations. As such, it should be more robust to noise (weakly matched pairs) in the training data and we expect a more graceful decline in performance.

Another classical method relevant to our inference task is canonical correlation analysis (CCA) [10, 11]. CCA can be used to find a pair of orthogonal projections for mapping data of each modality to the same space. The results for this approach are not presented herein for brevity and can be found in [2]. In terms of performance for the match detection task, the CCA-based method was very competitive with our dissimilarity-centric approach.

There have been many efforts toward solving the related problem of "manifold alignment". "Manifold alignment" seeks to find correspondences between disparate datasets in different conditions (which are sometimes referred to as "domains") by aligning their underlying manifolds. A common data setting found in the literature is the semi-supervised setting [9], where correspondences between two collections of observations are given and the task is to find correspondences between a new set of observations in each condition. The proposed solutions [6, 20, 21] follow the common approach of seeking a common latent space for multiple conditions such that the representations in this space (either projections or embeddings) of the observations match (are commensurate).

Wang and Mahedavan [20] suggest an approach that uses separate embeddings followed by Procrustes Analysis to find maps from the original disparate data to a commensurate space. Given a paired set of points, Procrustes Analysis [18] finds a linear transformation from one set of points to the other that minimizes sum of squared distances between pairs. In the problem considered in [20], the paired set of points are low-dimensional embeddings of kernel matrices. For the embedding step, they chose to use Laplacian Eigenmaps, though their algorithm allows for any appropriate embedding method.

Zhai et al. [21] solves an optimization problem with respect to two projection matrices for the observations in two domains. The energy function that is optimized contains three terms: two *manifold regularization terms* and one *correspondence preserving term*. The *manifold regularization terms* ensure that the local neighborhood of points are preserved in the low-dimensional space, by making use of the reconstruction error for Locally Linear Embedding [17]. The *correspondence preserving term* ensures that "matched" points are mapped to close locations in

the commensurate space.

Ham et al. [9] solve the problem in the semi-supervised setting by a similar approach, by optimizing a energy function that has three terms that are analogous to the terms in [21].

3 Problem Description

In the problem setting considered here, n different objects are measured under K different conditions (corresponding to, for example, K different sensors). We assume we begin with the data available in dissimilarity representation. These will be represented in matrix form as K $n \times n$ matrices $\{\Delta_k, k = 1, \ldots, K\}$. In addition, for each condition, dissimilarities between a new object and the previous n objects $\{\mathcal{D}_k, k = 1, \ldots, K\}$ are available. Under the null hypothesis, these new dissimilarities represent a *single* new object measured under K different conditions. Under the alternative hypothesis, the dissimilarities $\{\mathcal{D}_k\}$ represent *separate* new objects measured under K different conditions [15].

For the Wikipedia example presented in the introduction, two dissimilarity matrices are available: the dissimilarities between articles based on their textual content (Δ_1) and the dissimilarities between the vertices of the hyperlink graph (Δ_2). Various dissimilarity measures defined between pairs of graph vertices can be used to compute Δ_2. The dissimilarities between the new text document and the previous n text documents ($\mathcal{D}_1$) are also available, as well as the dissimilarities between a new vertex added to the graph and the previous n vertices ($\mathcal{D}_2$). The null hypothesis is that the new document and the vertex correspond to each other, while the alternative hypothesis is that they are not.

In order to derive a data representation where dissimilarities from disparate sources ($\{\mathcal{D}_k\}$) can be compared, the dissimilarities must be embedded in a commensurate metric space where the metric can be used to distinguish between matched and unmatched observations.

We do not assume the dissimilarity matrices have extra properties beyond the basic definition such as the metric property. While data from less disparate conditions should result in better performance in the inference task, our method does not restrict the type of dissimilarity measures that are used in each condition. Due to the disparateness of conditions and the dissimilarity measures used, the dissimilarity matrices $\{\Delta_k\}$ might have different scales of magnitude. We correct for this by normalizing the scale of each dissimilarity matrix. A reasonable choice for doing so is to divide each $\{\Delta_k\}$ by its Frobenius norm $\|\Delta_k\|_F$.

To embed multiple dissimilarities $\{\Delta_k\}$ into a commensurate space, an omnibus dissimilarity matrix $M \in \mathbb{R}^{nk \times nk}$ is constructed. Consider, for $K = 2$,

$$M = \begin{bmatrix} \Delta_1 & L \\ L^T & \Delta_2 \end{bmatrix} \tag{1}$$

where L is a matrix of imputed entries to be described later.

Remark For clarity of exposition, we will consider $K = 2$; the generalization to $K > 2$ is straightforward.

We define the commensurate space to be $\mathbb{R}^d$, where the embedding dimension d is pre-specified. The selection of d – model selection – is a task that requires much

attention and is beyond the scope of this article. We should emphasize the fact that the choice of d has an impact on most of the following work. For applications involving real data, we used the automatic dimensionality selection heuristic in [22]. This heuristic is derived from the assumption that the ordered eigenvalues $\{\lambda_i\}$ are drawn independently from two distributions from the same family $f(\lambda_i, \theta_1), f(\lambda_i, \theta_2)$ and optimizes the log-likelihood

$$l_q(\lambda) = \sum_{i=1}^{d} f(\lambda_i, \theta_1) + \sum_{i=d+1}^{n} f(\lambda_i, \theta_2)$$

with respect to d. Utilizing this heuristic provides an objective method to determine the "elbow" of the scree plot without requiring visualization and inspection by a data analyst. In the case domain knowledge is available for the data, it should be used to inform the selection of d. Otherwise, we recommend to future practitioners that they select the value of d such that the data in *both* modalities can be represented with small distortion in $\mathbb{R}^d$.

We use multidimensional scaling (MDS) [4, 8, 19] to embed the omnibus matrix in this space, and obtain a configuration of $2n$ embedded points $\{\hat{x}_{ik}; 1 \leq i \leq n; k \in \{1,2\}\}$ (which can be represented as $\hat{X}$, a $2n \times d$ matrix, where each row of the configuration matrix is the coordinate vector of an embedded point). The discrepancy between the interpoint distances of $\{\hat{x}_{ik}\}$ and the given dissimilarities in M is made as small as possible, as measured by an objective function

$$\sigma_W(\widetilde{X}; M) = \sum_{k_1 \in \{1,2\}; k_2 \in \{1,2\}} \sum_{1 \leq i_1 \leq n; 1 \leq i_2 \leq n} w_{i_1 i_2 k_1 k_2} (d(\hat{x}_{i_1 k_1}, \hat{x}_{i_2 k_2}) - M_{i_1 i_2 k_1 k_2})^2$$

with a $2n \times 2n$ weight matrix W. Each entry of W, $w_{i_1 i_2 k_1 k_2}$, correspond to an entry of M, $M_{i_1 i_2 k_1 k_2}$. In matrix form, $\hat{X} = \arg\min_{\widetilde{X}} \sigma_W(\widetilde{X}; M)$. This minimization problem is solved by the SMACOF algorithm [8].

Remark We will use x_{ik} to denote the (possibly notional) observation for the ith object in the kth condition, $\tilde{x}_{ik}$ to denote an argument of the objective function and $\hat{x}_{ik}$ to denote the arg min of the objective function. The notation for configuration matrices $(X, \widetilde{X}, \hat{X})$, whose each row corresponds to the embedding coordinates of an object, follows the same convention.

Given the omnibus matrix M and the $2n \times d$ embedding configuration matrix $\hat{X}$ in the commensurate space, the out-of-sample extension [12] developed for the raw-stress MDS variant will be used to embed the test dissimilarities $\mathcal{D}_1$ and $\mathcal{D}_2$. Once the test similarities are embedded as two points $(\hat{y}_1, \hat{y}_2)$ in the commensurate space, it is possible to compute the test statistic

$$\tau = d(\hat{y}_1, \hat{y}_2)$$

for the two "objects" represented by $\mathcal{D}_1$ and $\mathcal{D}_2$. For large values of τ, the null hypothesis will be rejected. If dissimilarities between matched objects are smaller than dissimilarities between unmatched objects with large probability, and the embeddings preserve this stochastic ordering, we could reasonably expect the test statistic to yield large power.

---

[2]which is based on the raw stress criterion $\sum_{1 \leq i_1 \leq n; 1 \leq i_2 \leq n} w_{i_1 i_2} (d(\hat{x}_{i_1}, \hat{x}_{i_2}) - \delta_{i_1 i_2})^2$

4 Fidelity and Commensurability

Regardless of the inference task, to expect reasonable performance from the embedded data in the commensurate space, it is necessary to pay heed to these two error criteria:

- Fidelity describes how well the mapping to commensurate space preserves the original dissimilarities. The *loss of fidelity* can be measured with the within-condition *fidelity error*, given by

$$\epsilon_{f(k)} = \frac{1}{\binom{n}{2}} \sum_{1 \leq i < j \leq n} (d(\widetilde{\boldsymbol{x}}_{ik}, \widetilde{\boldsymbol{x}}_{jk}) - \delta_{ijkk})^2.$$

  Here δ_{ijkk} is the dissimilarity between the ith object and the jth object where both objects are in the kth condition, and $\widetilde{\boldsymbol{x}}_{ik}$ is the embedded representation of the ith object for the kth condition; $d(\cdot, \cdot)$ is the Euclidean distance function.

- Commensurability describes how well the mapping to commensurate space preserves matchedness of matched observations. The *loss of commensurability* can be measured by the between-condition *commensurability error* which is given by

$$\epsilon_{c(k_1, k_2)} = \frac{1}{n} \sum_{1 \leq i \leq n; k_1 < k_2} (d(\widetilde{\boldsymbol{x}}_{ik_1}, \widetilde{\boldsymbol{x}}_{ik_2}) - \delta_{iik_1k_2})^2$$

  for conditions k_1 and k_2; $\delta_{iik_1k_2}$ is the dissimilarity between the ith object under conditions k_1 and k_2. Although the between-condition dissimilarities of the same object, $\delta_{iik_1k_2}$, are not available, it is reasonable to set these dissimilarities to 0 for all i, k_1, k_2. These dissimilarities correspond to diagonal entries of the submatrix L in the omnibus matrix M in equation (1). Setting these diagonal entries to 0 forces matched observations to be embedded close to each other.

While the above expressions for *fidelity* and *commensurability* errors are specific to the joint embedding of disparate dissimilarities, the concepts of fidelity and commensurability are general enough to be applicable to other dimensionality reduction methods for data from disparate sources.

In addition to fidelity and commensurability, there is the *separability* criteria: dissimilarities between unmatched observations in different conditions should be preserved (so that unmatched pairs are not embedded close together).

Let us now show how fidelity and commensurability errors can be made explicit in the objective function. Consider the weighted raw stress criterion ($\sigma_W(\cdot)$) which we choose as the objective function for the embedding of M with a weight matrix W. The entries of M are $\{M_{ijk_1k_2}\}$ for the available dissimilarities ($k_1 = k_2$). As the between-condition dissimilarities, $\{M_{ijk_1k_2}\}$ for $i \neq j$, are not available in general, the entries corresponding to the unavailable dissimilarities can be imputed[3]

---

[3]An effective imputation method is highly dependent on the nature of the disparate dissimilarities. In the case where the dissimilarities have the same order of magnitude and a high degree of matchedness, at the very least, the average of the two dissimilarities will have the right order of magnitude. It is also possible to disregard these dissimilarities altogether except those between matched observations in different conditions.

as $M_{ijk_1k_2} = \frac{M_{ijk_1k_1}+M_{ijk_2k_2}}{2}$. Then the objective function is

$$\sigma_W(\widetilde{X}; M) = \sum_{i \le j, k_1 \le k_2} w_{ijk_1k_2}(D_{ijk_1k_2}(\widetilde{X}) - M_{ijk_1k_2})^2. \tag{2}$$

Here, ijk_1k_2 subscript of a partitioned matrix refers to the entry in the ith row and j^{th} column of the sub-matrix in k_1^{th} row partition and k_2^{th} column partition, W is the weight matrix, $\widetilde{X}$ is the configuration matrix that is the argument of the stress function, $D(\cdot)$ is the matrix-valued function whose outputs are the Euclidean distances between the rows of its matrix argument. *Each of the individual terms in the sum (2) can be ascribed to fidelity, commensurability or separability.*

$$
\begin{aligned}
\sigma_W(\cdot; M) &= \sum_{i,j,k_1,k_2} \underbrace{w_{ijk_1k_2}(D_{ijk_1k_2}(\cdot) - M_{ijk_1k_2})^2}_{term_{i,j,k_1,k_2}} \\
&= \underbrace{\sum_{i=j,k_1<k_2} term_{i,j,k_1,k_2}}_{Commensurability} + \underbrace{\sum_{i<j,k_1=k_2} term_{i,j,k_1,k_2}}_{Fidelity} + \underbrace{\sum_{i<j,k_1<k_2} term_{i,j,k_1,k_2}}_{Separability} \quad .
\end{aligned}
\tag{3}
$$

Remark Due to the fact that data sources are "disparate", it is not obvious how a dissimilarity between an object in one condition and another object in another condition can be computed or defined in a sensible way. Although these unavailable dissimilarities appearing in the separability term can be imputed as mentioned, MDS variants such as weighted raw stress allows for disregarding the between-condition dissimilarities, by setting the corresponding weights in the raw stress function to 0. By doing so, we restrict our attention to the fidelity-commensurability tradeoff.

As mentioned in description of commensurability, we set the between-condition dissimilarities of the same object ($\{M_{iik_1k_2}\}$) to 0. Then the raw stress function can be written as

$$
\sigma_W(\widetilde{X}; M) = \underbrace{\sum_{i=j,k_1<k_2} w_{ijk_1k_2}(D_{ijk_1k_2}(\widetilde{X}))^2}_{Commensurability} + \underbrace{\sum_{i<j,k_1=k_2} w_{ijk_1k_2}(D_{ijk_1k_2}(\widetilde{X}) - M_{ijk_1k_2})^2}_{Fidelity} \quad .
$$

This motivates the naming of the omnibus embedding approach as Joint Optimization of Fidelity and Commensurability (JOFC).

The weights in the raw stress function allow us to address the question of the optimal tradeoff of fidelity and commensurability. Let $w \in (0,1)$. Setting the weights ($\{w_{ijk_1k_2}\}$) for the commensurability and fidelity terms to w and $1-w$, respectively, will allow us to control the relative importance of fidelity and commensurability terms in the objective function.

Let us denote the raw stress function with these simple weights by $\sigma_w(\widetilde{X}; M)$. With simple weighting, when $w = 0.5$, all terms in the objective function have the same weights. We will refer to this weighting scheme as *uniform weighting*. Uniform weighting does not necessarily yield the best fidelity-commensurability tradeoff in terms of subsequent inference.

Previous investigations of the JOFC approach [12,15] did not consider the effect of non-uniform weighting. Our thesis is that using non-uniform weighting in the objective function will allow for superior performance. That is, for a given inference task there is an optimal w for inference, denoted by w^*, and in general $w^* \neq 0.5$. In particular, as our inference task, we consider hypothesis testing, as in [15], and we let the area under the ROC curve, $AUC(w)$, be our measure of performance for any $w \in [0,1]$. In this setting, we show that $AUC(w)$ is continuous in the interval $(0,1)$, and hence $w^* = \arg\max_{w \in (\epsilon, 1-\epsilon)} AUC(w)$ exists for arbitrarily small ϵ. We demonstrate the potential practical advantage of our weighted generalization of JOFC via simulations.

5   Definition of w^*

Remark In our notation, (.) denotes either (m) or (u). In the former case, an expression refers to values under "matched" hypothesis, in the latter, the expression refers to values under "unmatched" hypothesis.

Let us denote the test dissimilarities $(\mathcal{D}_1, \mathcal{D}_2)$ by $(\mathcal{D}_1^{(m)}, \mathcal{D}_2^{(m)})$ under the "matched" hypothesis, and by $(\mathcal{D}_1^{(u)}, \mathcal{D}_2^{(u)})$ under the alternative. The out-of-sample embedding of $(\mathcal{D}_1^{(m)}, \mathcal{D}_2^{(m)})$ involves the augmentation of the omnibus matrix M, which consists of n matched pairs of dissimilarities, with $(\mathcal{D}_1^{(m)}, \mathcal{D}_2^{(m)})$. The resulting augmented $(2n+2) \times (2n+2)$ matrix has the form:

$$\Delta^{(m)} = \begin{bmatrix} M & \begin{matrix} \mathcal{D}_1^{(m)} & \vec{\mathcal{D}}_{NA} \\ \vec{\mathcal{D}}_{NA} & \mathcal{D}_2^{(m)} \end{matrix} \\ \begin{matrix} \mathcal{D}_1^{(m)T} & \vec{\mathcal{D}}_{NA}^T \\ \vec{\mathcal{D}}_{NA}^T & \mathcal{D}_2^{(m)T} \end{matrix} & \begin{matrix} 0 & \mathcal{D}_{NA} \\ \mathcal{D}_{NA} & 0 \end{matrix} \end{bmatrix}. \tag{4}$$

where the scalar $\mathcal{D}_{NA}$ and $\vec{\mathcal{D}}_{NA}$ (a vector of NAs that has length n) represent dissimilarities that are not available. In our JOFC procedure, these unavailable entries in $\Delta^{(m)}$ are either imputed using other dissimilarities that are available, or ignored in the embedding optimization. For a simpler notation, let us assume it is the former case. Also note that $\Delta^{(u)}$ has the same form as $\Delta^{(m)}$ where $\mathcal{D}_k^{(m)}$ is replaced by $\mathcal{D}_k^{(u)}$.

We define the dissimilarity matrices $\{\Delta^{(m)}, \Delta^{(u)}\}$ to be two matrix-valued random variables: $\Delta^{(m)} : \Omega \to \mathbf{M}_{(2n+2) \times (2n+2)}$ and $\Delta^{(u)} : \Omega \to \mathbf{M}_{(2n+2) \times (2n+2)})$ for the appropriate sample space (Ω).

Remark Suppose the objects in k^{th} condition can be represented as points in a measurable space Ξ_k, and the dissimilarities in k^{th} condition are given by a dissimilarity measure δ_k acting on pairs of points in Ξ_k. Assume $\mathcal{P}_{(m)}$ is the joint probability distribution over matched objects, while the joint distribution of unmatched objects $\{k = 1, \ldots, K\}$ is $\mathcal{P}_{(u)}$. Assuming the data are i.i.d., under the two hypotheses ("matched" and "unmatched", respectively), the $n+1$ pairs of objects are governed by the product distributions $\{\mathcal{P}_{(m)}\}^n \times \mathcal{P}_{(m)}$ and $\{\mathcal{P}_{(m)}\}^n \times \mathcal{P}_{(u)}$. The distributions of $\Delta^{(m)}$ and $\Delta^{(u)}$ are the induced probability distributions of these product distributions (induced by the dissimilarity measure δ_k applied to objects in k^{th} condition $\{k = 1, \ldots, K\}$).

We now consider the embedding of $\Delta^{(m)}$ and $\Delta^{(u)}$ with the criterion function $\sigma_W(\widetilde{X}; \Delta^{(\cdot)})$. The arguments of the function are $\widetilde{X} = \begin{bmatrix} \widetilde{\mathcal{T}} \\ \widetilde{y}_1^{(\cdot)} \\ \widetilde{y}_2^{(\cdot)} \end{bmatrix}$ where $\widetilde{\mathcal{T}}$ is the argument for the in-sample embedding of the first n pairs of matched points, and $\{\widetilde{y}_1^{(\cdot)}\}$ and $\{\widetilde{y}_2^{(\cdot)}\}$ are the arguments for the embedding coordinates of the matched or unmatched pair, and the omnibus dissimilarity matrix $\Delta^{(\cdot)}$ is equal to $\Delta^{(m)}$ (or $\Delta^{(u)}$) for the embedding of the matched (unmatched) pair. Note that we use the simple weighting scheme, so with a slight abuse of notation, we rewrite the criterion function as $\sigma_w(\widetilde{X}; \Delta^{(\cdot)})$ where w is a scalar parameter. The embedding coordinates for the matched or unmatched pair $\hat{y}_1^{(\cdot)}, \hat{y}_2^{(\cdot)}$ are given by

$$\hat{y}_1^{(\cdot)}, \hat{y}_2^{(\cdot)} = \underset{\widetilde{y}_1^{(\cdot)}, \widetilde{y}_2^{(\cdot)}}{\arg\min} \left[\underset{\widetilde{\mathcal{T}}}{\min}\, \sigma_w \left(\begin{bmatrix} \widetilde{\mathcal{T}} \\ \widetilde{y}_1^{(\cdot)} \\ \widetilde{y}_2^{(\cdot)} \end{bmatrix}, \Delta^{(\cdot)} \right) \right].$$

Remark Note that the in-sample embedding of $\widetilde{\mathcal{T}}$ is necessary but irrelevant for the inference task, hence the minimization with respect to $\widetilde{\mathcal{T}}$ is denoted by min instead $\arg\min$. It can be considered as a nuisance parameter for our hypothesis testing.

Remark Note also that all of the random variables following the embedding, such as $\{\hat{y}_k^{(\cdot)}\}$, are dependent on w; for the sake of simplicity, this will be suppressed in the notation.

Under reasonable assumptions, the embeddings $\Delta^{(m)} \to \{\hat{y}_1^{(m)}, \hat{y}_2^{(m)}\}$ and $\Delta^{(u)} \to \{\hat{y}_1^{(u)}, \hat{y}_2^{(u)}\}$ are measurable maps for all $w \in (0,1)$ [13]. Then, the distances between the embedded points are random variables and we can define the test statistic τ as $d(\hat{y}_1^{(m)}, \hat{y}_2^{(m)})$ under the null hypothesis and $d(\hat{y}_1^{(u)}, \hat{y}_2^{(u)})$ under the alternative. Under the null hypothesis, the distribution of the statistic is governed by the distribution of $\hat{y}_1^{(m)}$ and $\hat{y}_2^{(m)}$; under the alternative it is governed by the distribution of $\hat{y}_1^{(u)}$ and $\hat{y}_2^{(u)}$.

Then, the statistical power as a function of w is given by

$$\beta(w, \alpha) = 1 - F_{d\left(\hat{y}_1^{(u)}, \hat{y}_2^{(u)}\right)} \left(F_{d\left(\hat{y}_1^{(m)}, \hat{y}_2^{(m)}\right)}^{-1} (1 - \alpha) \right)$$

where F_Y denotes the cumulative distribution function of Y. The area under curve (AUC) measure as a function of w is defined as

$$AUC(w) = \int_0^1 \beta(w, \alpha)\, \mathrm{d}\alpha. \tag{5}$$

Although we might care about optimal w with respect to $\beta(w, \alpha)$ (with a fixed Type I error rate α), it will be more convenient to define w^* in terms of the AUC function.

Finally, define

$$w^* = \underset{w}{\arg\max}\, AUC(w).$$

Some important questions about w^* are related to the nature of the AUC function. While finding an analytical expression for the value of w^* is intractable, an estimate $\hat{w}^*$ based on estimates of $AUC(w)$ can be computed. For the Gaussian setting described in section 6.1, a Monte Carlo simulation is performed to find the estimate of $AUC(w)$ for different values of w.

5.1 Continuity of $AUC(\cdot)$

Let $T_0(w) = d(\hat{y}_1^{(m)}, \hat{y}_2^{(m)})$ and $T_a(w) = d(\hat{y}_1^{(u)}, \hat{y}_2^{(u)})$ denote the value of the test statistic under null and alternative distributions for the embedding with the simple weighting w. The AUC function can be written as

$$AUC(w) = P\left[T_a(w) > T_0(w)\right]$$

where $T_a(\cdot)$ and $T_0(\cdot)$ can be regarded as stochastic processes whose sample paths are functions of w. We will prove that $AUC(w)$ is continuous with respect to w. We start with this lemma from [16].

Lemma 1. *Let z be a random variable. The functional $g(z; \gamma) = P\left[z \geq \gamma\right]$ is upper semi-continuous in probability with respect to z. Furthermore, if $P\left[z = \gamma\right] = 0$, $g(z; \gamma)$ is continuous in probability with respect to z.*

Proof. Suppose z_n converges to z in probability. Then by definition, for any $\delta > 0$ and $\epsilon > 0$, $\exists N \in \mathbb{Z}^+$ such that for all $n \geq N$

$$Pr\left[|z_n - z| \geq \delta\right] \leq \epsilon.$$

The functional $g(z; \gamma)$ is non-increasing with respect to γ. Therefore, for $\delta > 0$, $g(z_n; \gamma) - g(z; \gamma) \geq g(z_n; \gamma) - g(z; \gamma - \delta)$. Furthermore, $g(z; \gamma)$ is left-continuous with respect to γ, so the difference between the two sides of the inequality can be made as small as desired.

$$
\begin{aligned}
g(z_n; \gamma) - g(z; \gamma - \delta) &= Pr\left[z_n \geq \gamma\right] - Pr\left[z \geq \gamma - \delta\right] & (6) \\
&\leq Pr\left[\{z_n \geq \gamma\} \backslash \{z \geq \gamma - \delta\}\right] & (7) \\
&\leq Pr\left[\{\{z_n \geq \gamma\} \backslash \{z \geq \gamma - \delta\}\} \cap \{z_n \geq z\}\right] & (8) \\
&= Pr\left[\{z_n - z \geq \delta\}\right] \leq \epsilon. & (9)
\end{aligned}
$$

Since ϵ and δ are arbitrary, $\limsup_{n \to \infty}(g(z_n; \gamma) - g(z; \gamma)) = 0$ for any $\delta > 0$, i.e. $g(z; \gamma)$ is upper semi-continuous.

By arguments symmetric to (6)-(9), we can show that

$$g(z; \gamma + \delta) - g(z_n; \gamma) \leq \epsilon. \qquad (10)$$

In addition, assume that $P\left[z = \gamma\right] = 0$. Then, $g(z; \gamma)$ is also right-continuous with respect to γ. Therefore, $g(z_n; \gamma) - g(z; \gamma) \leq g(z_n; \gamma) - g(z; \gamma + \delta)$ and the difference between the two sides of the inequality can be made as small as possible. Along with (10), this means that

$$\liminf_{n \to \infty}(g(z_n; \gamma) - g(z; \gamma)) = 0.$$

Therefore, $\lim_{n \to \infty} g(z_n; \gamma) = g(z; \gamma)$, i.e. $g(z; \gamma)$ is continuous in probability with respect to z. $\qquad \square$

Theorem 1. *Let $T(w)$ be a stochastic process indexed by w in the interval (0,1). Assume the process is continuous in probability (stochastic continuity) at $w = w_0$, i.e.*

$$\forall a > 0 \quad \lim_{s \to w_0} Pr\left[|T(s) - T(w_0)| \geq a\right] = 0 \tag{11}$$

for $w_0 \in (0, 1)$. Furthermore, assume that $Pr\left[T(w_0) = 0\right] = 0$.
  Then, $Pr\left[T(w) \geq 0\right]$ is continuous at w_0.

Proof. Consider any sequence $w_n \to w_0$. Let $z_n = T(w_n)$ and $z = T(w_0)$ and choose $\gamma = 0$. Since $T(w)$ is continuous in probability at w_0 and $Pr\left[T(w_0) = 0\right] = 0$, conditions for Lemma 1 hold, i.e. as $w_n \to w_0$, z_n converges in probability to $z = T(w_0)$. By Lemma 1, we conclude $g(T(w_n); 0) = Pr\left[T(w_n) \geq 0\right]$ converges to $g(T(w_0); 0)$. Therefore $g(T(w); 0)$ is continuous with respect to w. $\square$

Corollary 1. *If $Pr[T_a(w) - T_0(w) = 0] = 0$ and $T_a(w)$, $T_0(w)$ are continuous in probability for all $w \in (0, 1)$, then $AUC(w) = Pr\left[T_a(w) - T_0(w) > 0\right]$ is continuous with respect to w in the interval $(0, 1)$.*

Proof. Let $T(w) = T_a(w) - T_0(w)$. Then Theorem 1 applies everywhere in the interval (0,1). $\square$

In any closed interval that is a subset of $(0, 1)$, the AUC function is continuous and therefore attains its global maximum in that closed interval.

We do not have closed-form expressions for the null and alternative distributions of the test statistic τ (as a function of w), so we cannot provide a rigorous proof of the uniqueness of w^*. However, for various data settings, simulations always resulted in *unimodal* estimates for the AUC function which indicates a unique w^* value.

6   Simulation Results

6.1   Gaussian setting

Let n "objects" be represented by $\boldsymbol{\alpha}_i \sim^{iid} \mathcal{N}(\mathbf{0}, I_p)$. Let the $K = 2$ measurements for the ith object under the different conditions ($k \in (1, 2)$) be denoted by $\boldsymbol{x}_{ik} \sim^{iid} \mathcal{N}(\boldsymbol{\alpha_i}, \Sigma)$. The covariance matrix Σ is a positive-definite $p \times p$ matrix whose maximum eigenvalue is $\frac{1}{r}$. See Figure 1.

Dissimilarities (Δ_1 and Δ_2) for the omnibus embedding are the Euclidean distances between the measurements in the same condition.

The parameter r controls the variability between "matched" measurements. If r is large, it is expected that the distance between matched measurements $\boldsymbol{x}_{i1}$ and $\boldsymbol{x}_{i2}$ is stochastically smaller than $\boldsymbol{x}_{i1}$ and $\boldsymbol{x}_{i'2}$ for $i \neq i'$; if r is small, then dissimilarities between pairs of "matched" measurements and "unmatched" are less distinguishable. Therefore, a smaller value of r makes the decision problem harder, as the test statistic under null and alternative will have highly similar distributions, resulting in higher rate of errors or tests with smaller AUC measure.
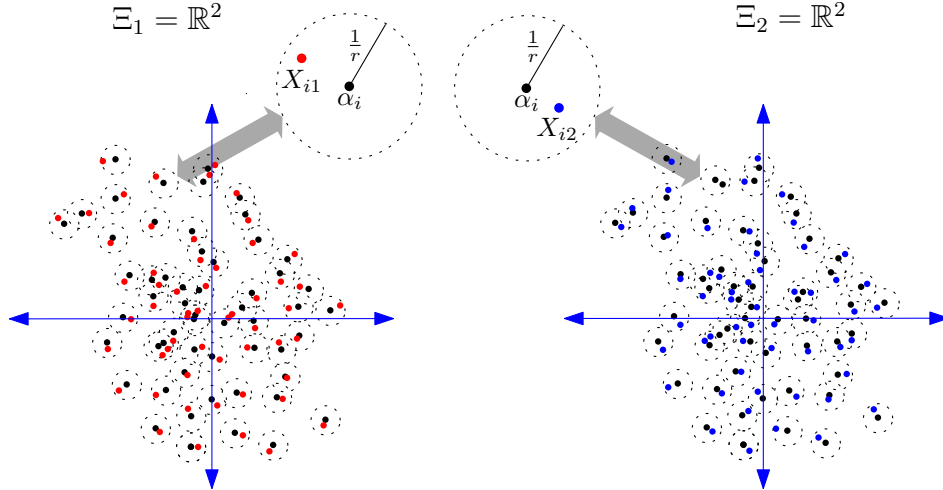
Figure 1: For the Gaussian setting (Section 6.1), the objects can be represented by $\boldsymbol{\alpha_i}$ which are two-dimensional random vectors denoted by black points and distributed as $\mathcal{N}(\mathbf{0}, I_p)$. The dashed lines show the equal probability contours for each $\boldsymbol{\alpha_i}$. Since the measurements in the two conditions and the original object are in the same space ($\mathbb{R}^2$), $\boldsymbol{\alpha_i}$ can be shown along with the measurements $\boldsymbol{x}_{ik}$ which are denoted by red ($k = 1$) and blue ($k = 2$) points respectively.

6.2 Simulation

We generate the training data of matched sets of measurements according to the Gaussian setting. Dissimilarity representations are computed from pairwise Euclidean distances of these measurements. We also generate a set of matched pairs and unmatched pairs of measurements for testing using the same Gaussian setting. Following the out-of-sample embedding of the test dissimilarities we compute test statistics for matched and unmatched pairs. This allows us to compute the empirical power at different values of α (Type I error rate) and the empirical AUC measure.

The measurements for the Gaussian setting are vectors in p-dimensional Euclidean space (p=5). For $nmc = 400$ Monte Carlo replicates, $n = 150$ matched training pairs and $m = 250$ matched and unmatched test pairs (generated according to the Gaussian setting) were generated. Using the resulting test statistic values for matched and unmatched test pairs, the AUC measure was computed for different w values along with the average of the power (β) values at different values of α.

The plot in Figure 2 shows the β vs α curves for different values of w. It is clear from the plot that w has a significant effect on statistical power (β). There are several w values in the range $(0.85, 0.95)$ that result in power values that are close to optimal, and statistical power declines as $w \to 0$ or as $w \to 1$. Also, note that the estimate of the optimal w^* has an AUC measure higher than that of w=0.5 (uniform weighting) which confirms our thesis that non-uniform weighting could result in larger statistical power. This finding was confirmed using data generated according to the Gaussian setting with different sets of parameters.

In Figure 3, $\beta(w)$ is plotted against w for fixed values of α. Here the effect of
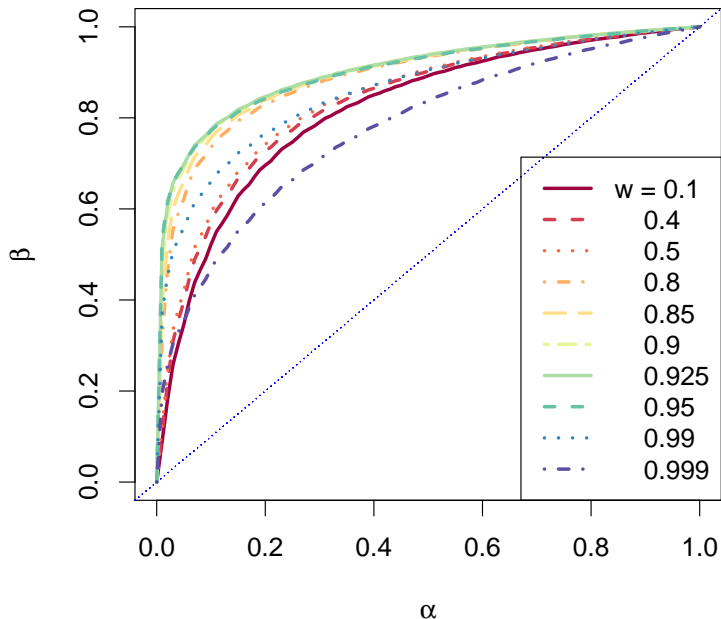
Figure 2: β vs α for different choices of w

w	0.1	0.4	0.5	0.8	0.85	0.9	0.91	0.92
mean	0.8147	0.8308	0.8381	0.8884	0.8961	0.9021	0.9030	0.9037
SE	0.0640	0.0574	0.0537	0.0258	0.0226	0.0209	0.0206	0.0210
w	0.925	0.93	0.94	0.95	0.96	0.99	0.999	
mean	0.9040	0.9036	0.9034	0.9022	0.8995	0.8576	0.7746	
SE	0.0209	0.0209	0.0210	0.0210	0.0217	0.0270	0.0474	

Table 1: Mean and standard error of $AUC(w)$ for 400 Monte Carlo replicates.

w on power can be seen more clearly: for all three values of α, $\beta(w)$ increases as w approaches a value in the range (0.91,0.96) and then starts to decrease. We see this trend for different values of α which is consistent with our conjecture that the AUC function, which is defined in equation (5), is unimodal.

The average AUC measure for these $nmc = 400$ Monte Carlo replicates are in Table 1.

The value of w which results in the highest AUC measure is different for each Monte Carlo replicate. The number of replicates for which a particular w value led to the highest AUC measure is shown in the bar chart in Figure 5. Only the non-zero counts are shown in the plot. The estimate $\hat{w}^*$ can be chosen as 0.925, as it is the mode of w^* estimates from all replicates. We should note that the AUC function is very flat in the interval $(0.85, 0.99)$, and it is possible that the difference between the largest value of the AUC measure and the next largest is very small for any replicate.

We also compared our approach with two 3-way MDS-based methods, IDIOSCAL

13
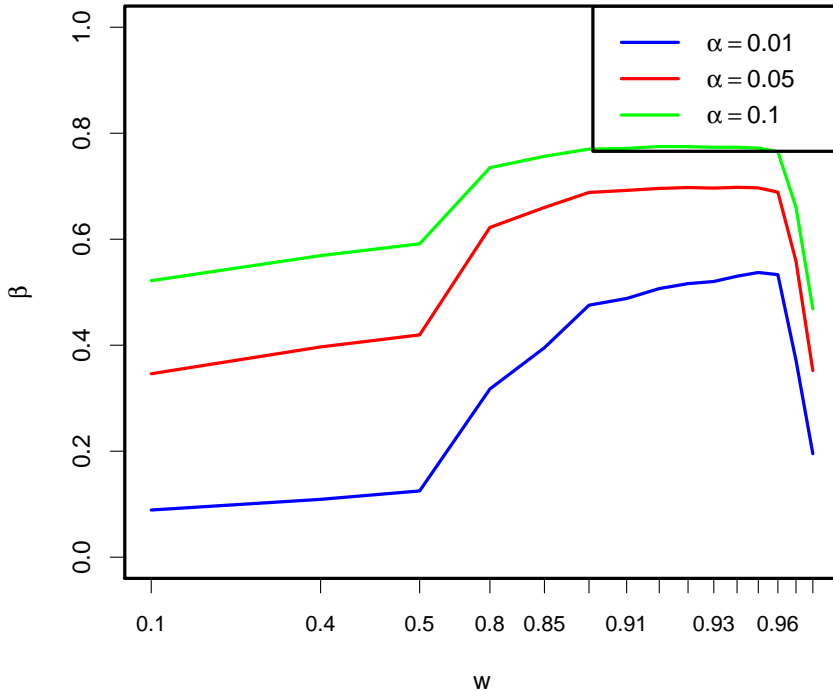
Figure 3: β vs w plot for different choices of α

and INDSCAL, for the Gaussian setting. Our JOFC approach with the best w value outperforms both as shown in Figure 6. The ROC curves for INDSCAL and IDIOSCAL are indistinguishable as the estimated transformation matrix from group space to configuration spaces should not deviate from the identity matrix too much[4]. Thus, both methods are equivalent in this Gaussian setting with identity mapping between the two conditions.

7   Experiments with multimodal data

To test our approach, we will use a real dataset with two disparate conditions. The dissimilarities in the two conditions[5] are derived from brain fMRI images collected from $n = 42$ patients, and from the personality scores of those patients [3]. We wish to discover commensurate mappings for data from the two domains and match detection provides a simple test problem for measuring the commensuracy of the joint embedding.

For each replicate of our experiment, we randomly sample two matched pairs of rows from the two dissimilarity matrices. We use one of the matched pairs as our matched test example. We also use one row of each pair (say, first row from the first condition and second row from the second condition) as the unmatched test

---

[4]For the configuration space of dimension p, INDSCAL restricts the transformation matrix to $p \times p$ diagonal matrices while IDIOSCAL allows for any $p \times p$ square matrix.

[5]The dissimilarity data are available in `http://www.cis.jhu.edu/~parky/CGP/cgp.html`.
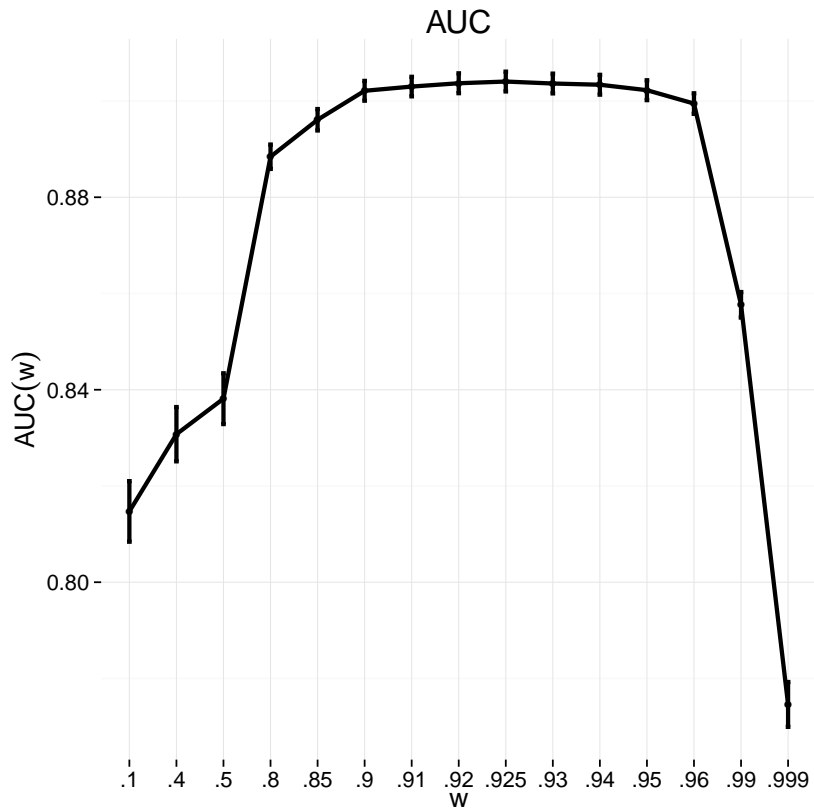
Figure 4: Mean and SE of $AUC(w)$ values for 400 Monte Carlo replicates.
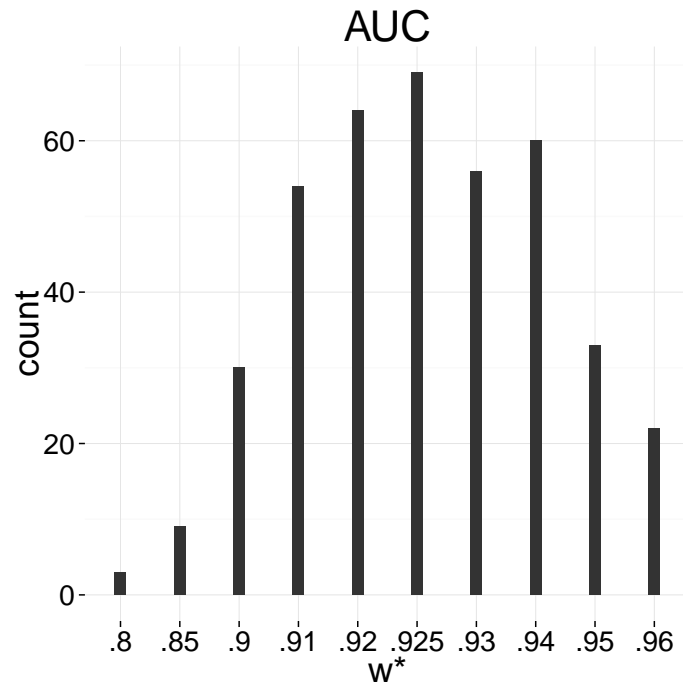
Figure 5: Frequency plot of w^* estimates for 400 replicates.
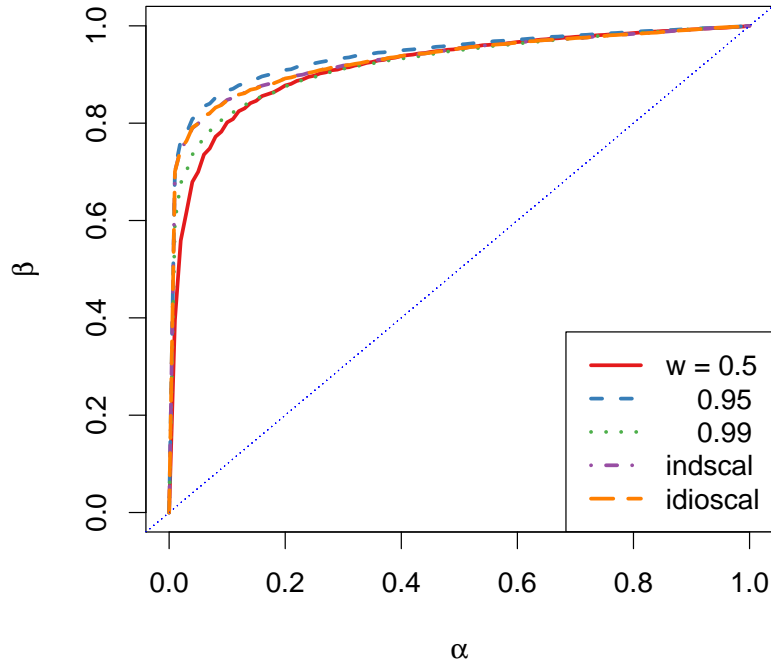
Figure 6: β vs α for JOFC with different choices of w and for INDSCAL method

example. The remaining rows/columns form the in-sample dissimilarity matrices Δ_1, Δ_2. We jointly embed these 40×40 dissimilarity matrices. The test examples are then OOS-embedded to compute the test statistic for match detection. The critical value for the decision to reject the null hypothesis can be computed by a boot-strapping method, i.e. repeatedly sampling two matched row pairs of Δ_1 and Δ_2 to OOS-embed, so that the test statistic under the null and alternative hypothesis can be computed[6].

The ROC curve in figure 7 shows the performance of the JOFC approach. We also show the results for the PrM method which uses Procrustes matching of separate MDS embeddings for a commensurate representation. For low α values, which are typically of more interest, the JOFC approach out-performs PrM. We chose $\alpha = 0.05$ and used critical values computed via bootstrapping in each replicate of the experiment. The effective size averaged over the replicates is 0.04, the average effective power is 0.18.

8 Conclusion

We investigated the tradeoff between fidelity and commensurability and its relation to the weighted raw stress criterion for MDS. For hypothesis testing as the exploitation task, different values of the tradeoff parameter w were compared in

---

[6]The common bootstrapping method of resampling observations is inappropriate in this case, since the dissimilarity matrices would have rows of zeroes.
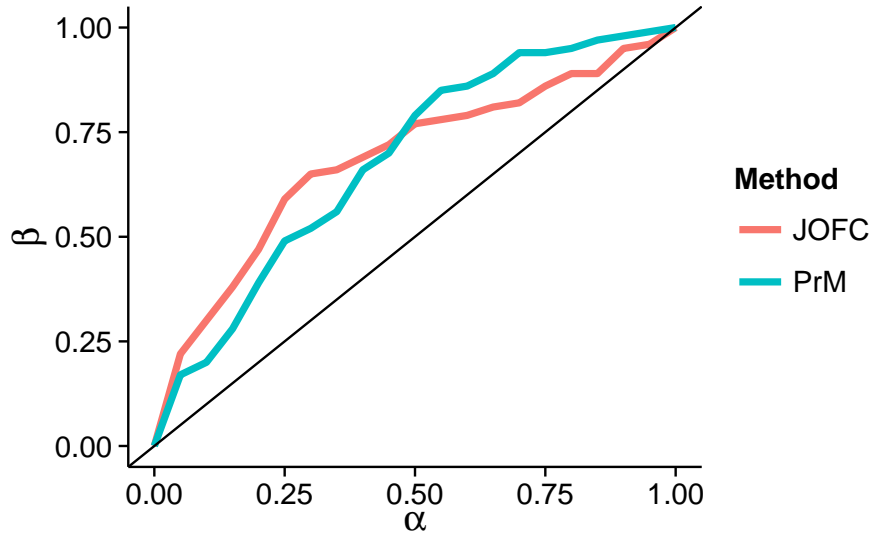
Figure 7: ROC curve for multimodal dataset: MRI/cognitive test

terms of testing power. The results indicate that when doing a joint optimization, one should consider an optimal compromise point between fidelity and commensurability, which corresponds to an optimal weight w^* of the weighted raw stress criterion in contrast to the uniform weighting. We consider an estimate of w^* chosen from a finite set of w values for a data generated according to the Gaussian setting. We test the applicability of the JOFC approach for a real multimodal dataset and find it provides satisfactory performance.

References

[1] Hervé Abdi, Dominique Valentin, Alice J O'Toole, and Betty Edelman. DIS-TATIS: The analysis of multiple distance matrices. In *Proceedings of the IEEE Computer Society: International Conference on Computer Vision and Pattern Recognition*, pages 42–47, 2005.

[2] Sancar Adali. *Joint Optimization of Fidelity and Commensurability for Manifold Alignment and Graph Matching*. PhD thesis, The Johns Hopkins University, 2014.

[3] Jonathan S. Adelstein, Zarrar Shehzad, Maarten Mennes, Colin G. DeYoung, Xi-Nian Zuo, Clare Kelly, Daniel S. Margulies, Aaron Bloomfield, Jeremy R. Gray, Xavier Castellanos, and Michael Milham. Personality is reflected in the brain's intrinsic functional architecture. *PLoS ONE*, 6(11):e27633, 11 2011.

[4] Ingwer Borg and Patrick Groenen. *Modern Multidimensional Scaling: Theory and Applications*. Springer, 1997.

[5] J. Douglas Carroll and Jih-Jie Chang. Analysis of individual differences in multidimensional scaling via an n-way generalization of "Eckart-Young" decomposition. *Psychometrika*, 35(3):283–319, 1970.

[6] Brent Castle, Michael W. Trosset, and Carey E. Priebe. A nonmetric embedding approach to testing for matched pairs. (TR-11-04), October 2011.

[7] Jacques Commandeur and Willem J. Heiser. Mathematical Derivations in the Proximity Scaling (PROXSCAL) of Symmetric Data Matrices. Technical Report Research Report RR-93-04, Department of Data Theory, Leiden University, 1993.

[8] Jan de Leeuw. Applications of convex analysis to multidimensional scaling. In *Recent Developments in Statistics*, 1977.

[9] Jihun Ham, Daniel D. Lee, and Lawrence K. Saul. Semisupervised alignment of manifolds. In *Proceedings of the Annual Conference on Uncertainty in Artificial Intelligence, Z. Ghahramani and R. Cowell, Eds*, volume 10, pages 120–127, 2005.

[10] David R. Hardoon, Sandor R. Szedmak, and John R. Shawe-Taylor. Canonical correlation analysis: An overview with application to learning methods. *Neural Computation*, 16:2639–2664, December 2004.

[11] Harold Hotelling. Relations between two sets of variates. *Biometrika*, 28(3-4):321–377, 1936.

[12] Zhiliang Ma. *Disparate information fusion in the dissimilarity framework*. PhD thesis, The Johns Hopkins University, 2010.

[13] Wojciech Niemiro. Asymptotics for M-estimators defined by convex minimization. *The Annals of Statistics*, 20(3):pp. 1514–1533, 1992.

[14] E. Pekalska and R.P.W. Duin. *The dissimilarity representation for pattern recognition: foundations and applications*. Series in machine perception and artificial intelligence. World Scientific, River Edge, NJ, 2005.

[15] Carey E. Priebe, David J. Marchette, Zhiliang Ma, and Sancar Adali. Manifold matching: Joint optimization of fidelity and commensurability. *Brazilian Journal of Probability and Statistics*, 27(3):377–400, August 2013.

[16] E. Raik. On the stochastic programming problem with the probability and quantile functionals. *Izvestia Akademii Nauk Estonskoy SSR. Phys and Math.*, 21(2):142–148, 1972.

[17] Sam T. Roweis and Lawrence K. Saul. Nonlinear dimensionality reduction by locally linear embedding. *Science*, 290(5500):2323–2326, 2000.

[18] Robin Sibson. Studies in the Robustness of Multidimensional Scaling: Procrustes Statistics. *Journal of the Royal Statistical Society. Series B (Methodological)*, 40(2):234–238, 1978.

[19] Warren. Torgerson. Multidimensional scaling: I. theory and method. *Psychometrika*, 17:401–419, 1952.

[20] C. Wang and S. Mahadevan. Manifold alignment using Procrustes analysis. In *Proceedings of the 25th international conference on Machine learning - ICML '08*, pages 1120–1127, New York, New York, USA, 2008. ACM Press.

[21] D. Zhai, B. Li, H. Chang, S. Shan, X. Chen, and W. Gao. Manifold alignment via corresponding projections. In *Proceedings of the British Machine Vision Conference*, pages 3.1–3.11. BMVA Press, 2010. doi:10.5244/C.24.3.

[22] Mu Zhu and Ali Ghodsi. Automatic dimensionality selection from the scree plot via the use of profile likelihood. *Computational Statistics & Data Analysis*, 51(2):918–930, 2006.